HAL open science

Comment on "Rethinking the Lower Bound on Aerosol Radiative Forcing"

Jan Kretzschmar, Marc Salzmann, Johannes Mülmenstädt, Olivier Boucher, Johannes Quaas

To cite this version:

Jan Kretzschmar, Marc Salzmann, Johannes Mülmenstädt, Olivier Boucher, Johannes Quaas. Comment on "Rethinking the Lower Bound on Aerosol Radiative Forcing". Journal of Climate, 2017, 30, pp.6579-6584. 10.1175/JCLI-D-16-0668.1 . insu-03727057

HAL Id: insu-03727057

https://insu.hal.science/insu-03727057

Submitted on 27 Jul 2022

HAL is a multi-disciplinary open access archive for the deposit and dissemination of scientific research documents, whether they are published or not. The documents may come from teaching and research institutions in France or abroad, or from public or private research centers.

L'archive ouverte pluridisciplinaire **HAL**, est destinée au dépôt et à la diffusion de documents scientifiques de niveau recherche, publiés ou non, émanant des établissements d'enseignement et de recherche français ou étrangers, des laboratoires publics ou privés.

Distributed under a Creative Commons Attribution 4.0 International License

CORRESPONDENCE

Comment on "Rethinking the Lower Bound on Aerosol Radiative Forcing"

JAN KRETZSCHMAR, MARC SALZMANN, AND JOHANNES MÜLMENSTÄDT

Institute for Meteorology, Universität Leipzig, Leipzig, Germany

OLIVIER BOUCHER

Laboratoire de Météorologie Dynamique, Université Pierre et Marie Curie/CNRS, Paris, France

JOHANNES QUAAS

Institute for Meteorology, Universität Leipzig, Leipzig, Germany

(Manuscript received 7 September 2016, in final form 4 April 2017)

ABSTRACT

In an influential and interesting study, Stevens (2015) suggested that the global and also Northern Hemispheric warming during the early industrial period implies that the effective radiative forcing (F_{aer}) by anthropogenic aerosols in the year 2000 compared to 1850 cannot be more negative than $-1.0\,\mathrm{W\,m^{-2}}$. Here results from phase 5 of the Coupled Model Intercomparison Project are analyzed and it is shown that there is little relationship between F_{aer} and the warming trend in the early industrial period in comprehensive climate models. In particular, some models simulate a warming in the early industrial period despite a strong (very negative) F_{aer}. The reason for this difference in results is that the global-mean log-linear scaling of F_{aer} with anthropogenic sulfur dioxide emissions introduced and used by Stevens tends to produce a substantially larger aerosol forcing compared to climate models in the first half of the twentieth century, when SO_2 emissions were concentrated over smaller regions. In turn, it shows smaller (less negative) F_{aer} in the recent period with comparatively more widespread SO_2 emissions.

1. Introduction

Quantitative understanding of climate change during the industrial era suffers from a highly uncertain effective radiative forcing (radiative forcing plus adjustments) due to anthropogenic aerosols, F_{aer} (Boucher et al. 2013). Stevens (2015, hereinafter S15) proposed that the temporal and spatial characteristics of the observed warming since preindustrial times provide a powerful constraint on the total anthropogenic aerosol forcing. We follow S15 and assume that warming during the 1860–1950 and 1920–50 periods is largely driven by anthropogenic forcings, although climate internal variability and natural forcings should be accounted for properly. S15 argues that one can exploit the fact that due to their long lifetime, greenhouse gases accumulate in the atmosphere whereas, with a lifetime of about 1 week, the forcing by anthropogenic aerosols is closely related to the emissions. As such, the greenhouse gas forcing increases gradually over time, but the aerosol forcing shows more spatial and temporal fluctuations. Based on process considerations, S15 develops a simple, zero-dimensional model for the global-mean aerosol forcing that combines a linear scaling of anthropogenic global-mean sulfur dioxide emissions to represent the radiative forcing (RF) due to aerosol–radiation interactions and a logarithmic scaling of the same quantity to represent the RF due to aerosol–cloud interactions. The logarithmic contribution is of large importance for the constraint, since it implies that anthropogenic sulfur emissions had a relatively larger impact in the early

Denotes content that is immediately available upon publication as open access.

Corresponding author: Johannes Quaas, johannes.quaas@uni-leipzig.de

DOI: 10.1175/JCLI-D-16-0668.1

© 2017 American Meteorological Society. For information regarding reuse of this content and general copyright information, consult the AMS Copyright Policy (www.ametsoc.org/PUBSReuseLicenses).

Unauthenticated | Downloaded 07/27/22 06:04 AM UTC

industrial period than at later times, when atmospheric sulfate concentrations were already high. The reason to consider a logarithmic scaling is the fact that further increases in cloud condensation nuclei (CCN) concentrations become less effective as CCN concentrations increase. On the one hand, there are more CCN competing for the water vapor, reducing the activation, and on the other hand, cloud albedo is a nonlinear function of cloud optical thickness.

The link between the observed warming and aerosol forcing had been demonstrated earlier (e.g., Schwartz 2012; Forster et al. 2013) and was refined by S15 to focus on the early warming period (until 1950). S15 argues that since globally, as well as for the Northern Hemisphere alone, a steady warming was observed, the aerosol forcing could not have more than offset the greenhouse gas forcing either globally or above the Northern Hemisphere.

The study of Rotstayn et al. (2015) touched on the results of S15 by analyzing climate model simulations of phase 5 of the Coupled Model Intercomparison Project (CMIP5; Taylor et al. 2012), which called the argument in S15 into question. Rotstayn et al. (2015) suggested—and S15 discussed this argument as well—that three-dimensional models (unlike the global-mean model used by S15) allow for transport of aerosol away from pollution sources (several 1000 km considering a lifetime of 1 week and a horizontal wind speed of $10\,\mathrm{m\,s^{-1}}$) into pristine regions. In consequence, the forcing due to aerosol–cloud interactions saturates less quickly than would be the case if aerosols accumulated in the source regions only. Thus, the forcing may scale more or less linearly with emissions for many regions. This is in particular the case for marine clouds downwind of the continents, which are thought to contribute most to the global effective forcing due to aerosol–cloud interactions (e.g., Quaas et al. 2008).

2. Results

Figure 1 shows the relationship (or lack of relationship) between the warming trend from 1860 to 1950, as well as 1920 to 1950, from the historical simulations of CMIP5 averaged globally and over the Northern Hemisphere, respectively, as a function of global-mean F_{aer} diagnosed from the difference between the CMIP5 SSTClimAerosol and SSTClim simulations [see Taylor et al. (2012) for a description of these standardized simulations]. The correlation coefficients between F_{aer} and temperature trends are 0.04 and 0.06 globally for the 1860–1950 and 1920–50 periods, respectively, and 0.19 and 0.10 for the Northern Hemisphere. For the period 1860 to 1950, the models simulate global warming of between +0.2° and +0.45°C, encompassing the observed value of +0.3°C. The natural variability, as evident by the ensemble spread in warming for a given model, is rather large. For each given model (except one), the range from the ensemble historical simulations encompasses the observed value of the global warming for the period. As Forster et al. (2013) noted earlier, the CMIP5 models do not necessarily perfectly match the observed warming, which allows us to explore the potential relationship (or lack of thereof) between simulated temperature and F_{aer} (see also Rotstayn et al. 2015). The Northern Hemisphere analysis suggests that models with an F_{aer} less negative than $-0.8\,\mathrm{W\,m^{-2}}$ tend to show a too strong warming, and the model with an F_{aer} of $-1.6\,\mathrm{W\,m^{-2}}$ shows a warming that is too weak for most ensemble members, but the large intermodel variations prevent a strong emergent constraint. Note that this finding that models with a rather strong F_{aer} often compare well to observations is not restricted to the early warming period. Ekman (2014) compared the warming trend 1965–2004 in the models to observations for different subregions of the globe and found that on average NorESM, CSIRO, GFDL-CM3, and HadGEM, which are models with strong F_{aer}, performed best. This is consistent with the study by Cherian et al. (2014), which investigated the surface solar radiation trends over Europe from 1990 to 2005 and found that HadGEM, CSIRO, and GFDL-CM3 were closest to the observed trend. Wang (2015) also found that a group of models including NorESM, CSIRO, GFDL-CM3, and HadGEM was better at reproducing observed patterns of precipitation changes, compared with a group of models that included a less advanced description of aerosol–cloud interactions. When considering the short period 1920 to 1950, most models show less warming than the observations globally and also, to a lesser extent, for the Northern Hemisphere, but are consistent with the observations. The main conclusion from Fig. 1 is that no lower bound on F_{aer} can be inferred from the early anthropogenic warming on the basis of available climate models.

To better understand why the analysis of S15 fails when applied to climate models, we compare the F_{aer} from his global-mean model to estimates from climate models. Since no systematic diagnostic of the transient F_{aer} is available in CMIP5 [see discussion in Pincus et al. (2016)], we follow the approach of Forster et al. (2013) and Rotstayn et al. (2015) to estimate it for the subset of models analyzed in Fig. 1 for which an additional simulation with only anthropogenic aerosol varying in time over the historical period (historicalAA; Taylor et al. 2012) is available. Using this approximation to the transient F_{aer} in its global mean in relationship to anthropogenic SO_2 emissions (Fig. 2), we find an

Unauthenticated | Downloaded 07/27/22 06:04 AM UTC

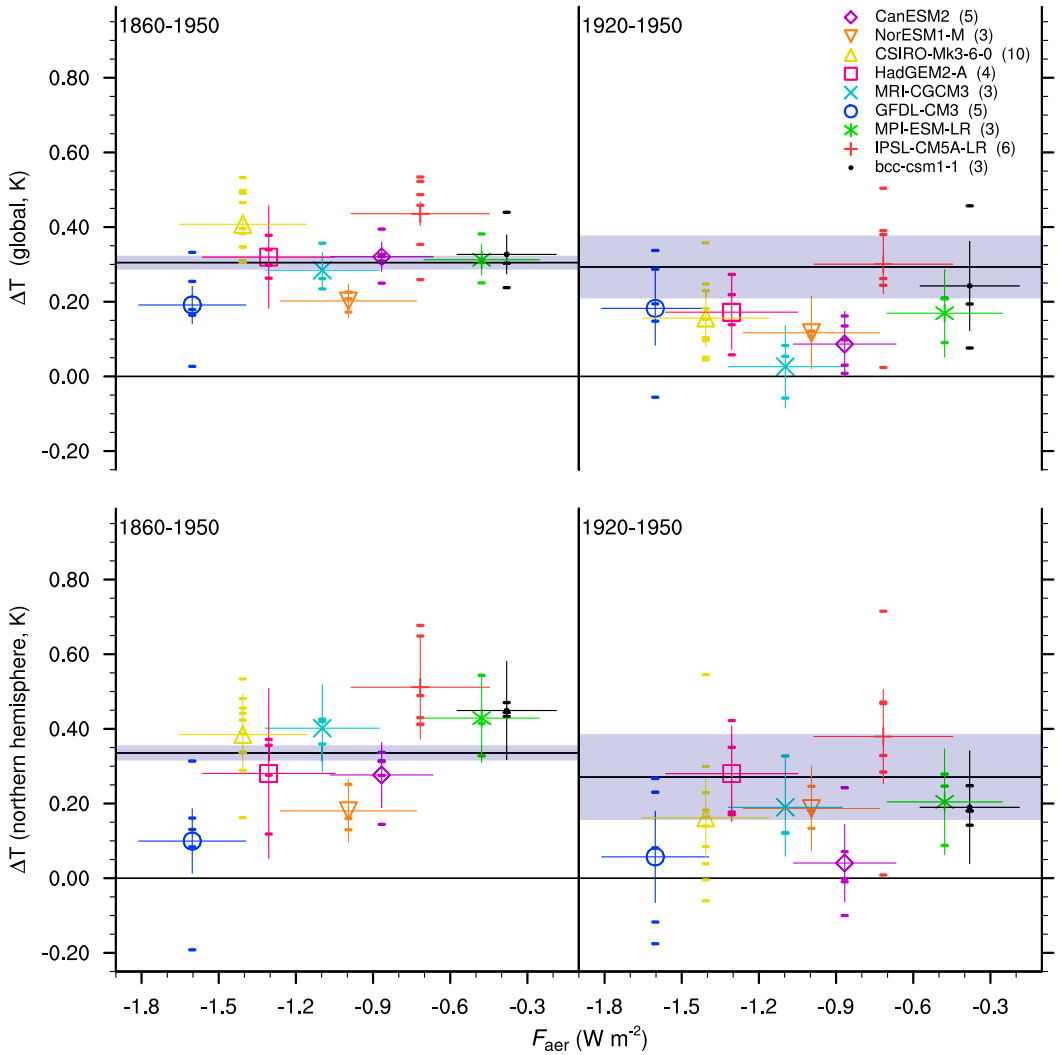

FIG. 1. Scatterplot of the near-surface temperature change (assessed from the linear trend computed from the annual global/hemispheric mean temperatures multiplied by the period duration) for the periods (left) 1860–1950 and (right) 1920–50, where the (top) global-mean and (bottom) Northern Hemisphere–only temperature was used, vs the aerosol effective radiative forcing (x axis, diagnosed in as global mean from the SSTClimAerosol minus SSTClim simulations with 2000 and 1850 aerosol and aerosol precursor emissions, respectively, all else being equal). The symbols are from the ensemble means for different climate models in the CMIP5 ensemble, with the error bar from the temporal standard deviation of the F_{aer} (horizontal) and the uncertainty of the temperature change from variations in start and end years of the time period by ±5 yr (vertical). Small bars indicate the temperature change diagnosed from individual ensemble members of the historical simulation; the number of ensemble members available for each model is given in brackets on the upper right. The horizontal black line is the estimate of the temperature trends from the Hadley Centre/Climate Research Unit temperature observations datasets (HadCRUT4.4; Morice et al. 2012) with the uncertainty as a gray shaded area defined as for the models.

approximately linear, or very slightly sublinear, scaling. When considering continental-scale regions (Fig. 2b), the curves are more bent; that is, they show a more nonlinear behavior (see below for more analysis). Note that the climate models assessed here parameterize the behavior of the cloud response to aerosols as being logarithmic at a local level. While the global-mean behavior is broadly consistent with the S15 model, the latter shows substantially larger aerosol forcing in the 1900–50 period compared to the four climate models; the opposite is found for 2000 for which F_{aer} is assessed (Table 1). Please note that in the models there is a systematic difference between the F_{aer} diagnosed from the dedicated simulations and the one estimated from the transient simulations, the former being about 25% stronger [see Sherwood et al. (2015) for a discussion of

Unauthenticated | Downloaded 07/27/22 06:04 AM UTC

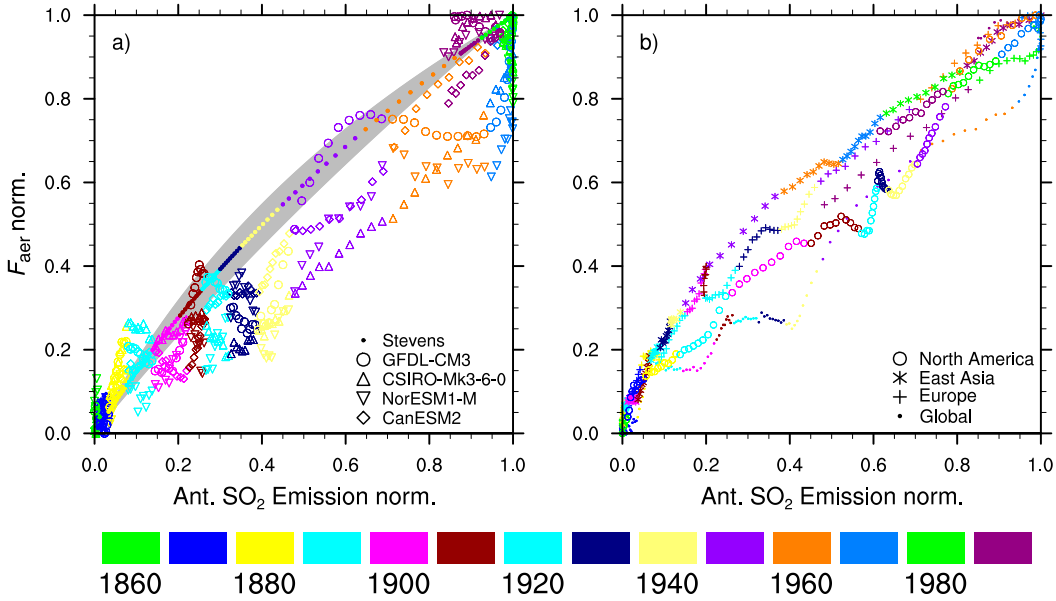

FIG. 2. Scatterplot of the transient annual-mean F_{aer} diagnosed as in Forster et al. (2013) for a subset of four models analyzed in Fig. 1 for which the historicalAA simulations and emission diagnostics were available vs the global annual mean anthropogenic sulfur dioxide emission rate. Both F_{aer} and SO_2 emissions are computed relative to 1860 and normalized to their maximum value for each model. A running mean of 11 years is applied. The different symbols are for four different GCMs as well as for the global-mean model developed and applied by S15, and the color depicts the years of the 1860–2005 simulation period (in steps of 10 years starting in 1860). The gray shading shows the $\pm 2\sigma$ range by the variants of the S15 model; the symbols for the S15 correspond to the median model. Shown are (left) global-mean values for individual models and the S15 model, and (right) the average over the four models for three different continent-scale regions and the global mean.

this difference]. S15 simulates for 1950 (average 1945–55) an F_{aer} that already is 65% (62%) of the F_{aer} in 2000 (in the transient 1995–2005 period), whereas this ratio is only 34% (41%) in the climate models. The conclusion is that the S15 model shows a behavior that is substantially more logarithmic than the comprehensive models. A plausible reason for this is the large heterogeneity of the aerosol forcing as shown in Fig. 3. While the forcing was concentrated in relatively small regions in the first half of the twentieth century, it is much more spread out at the end of the twentieth century. It is only in small regions, thus, that the forcing is rather logarithmic in the climate models (cf. Fig. 2b), while in its global mean the forcing to a good approximation scales linearly with the anthropogenic sulfur emissions. In the early anthropogenic warming period, and toward the end of the twentieth century, emissions of carbonaceous aerosol, which is not considered in the S15 model, are also rather important (Lamarque et al. 2010; Stevens et al. 2017) and may be a reason for the more linear response in the complex models (Ghan et al. 2013). Carbonaceous aerosols not only have a temporal evolution that may be different from that of sulfate aerosols, but they also contribute a positive radiative forcing that

TABLE 1. F_{aer} in 2000 (from the SSTClimAerosol and SSTClim) and estimated global-mean effective RF for the early twentieth century (from the historical and historicalAA simulations), for the four models analyzed in Fig. 1 (the values from the transient simulation are the arithmetic averages in a 10-yr period centered on the year indicated) and the S15 model.

Model	F_{aer} (W m^{-2})	2000 (W m^{-2})	1950 (W m^{-2})	1950 (% of F_{aer})	1950 (% of 2000)
CanESM2	−0.87	−0.85	−0.46	53	54
NorESM1-M	−1.00	−0.80	−0.26	26	33
CSIRO-Mk3.6.0	−1.41	−0.96	−0.30	21	31
GFDL CM3	−1.60	−1.23	−0.54	34	44
Average GCMs	−1.22	−0.96	−0.39	34	41
S15	−0.81	−0.81	−0.50	62	62

Unauthenticated | Downloaded 07/27/22 06:04 AM UTC

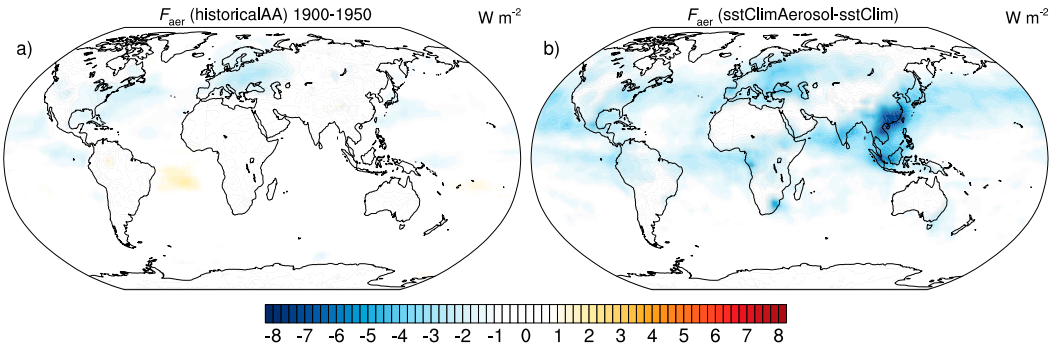

FIG. 3. Geographical, temporal-mean distribution of F_{aer} (W m^{-2}) relative to 1860 averaged over the four GCMs shown in Fig. 2 for (right) year 2000 (SSTClimAerosol − SSTClim) and (left) averaged over the 1900–50 period [method of Forster et al. (2013), using the historicalAA simulation].

may have masked some of the earlier negative aerosol forcing.

3. Discussion

The discrepancies between the results presented here and those from S15 are due to the difference in the models applied. In his paper, S15 argues that comprehensive models may not be trusted to realistically simulate F_{aer}, since many of the relevant processes are poorly constrained. In turn, it may be questioned whether the simple global-mean model of S15 is superior to the comprehensive models assessed here. As such, further research is necessary. Dedicated climate model studies, such as those proposed by Pincus et al. (2016), may be instrumental. In addition, it is imperative to aim at an observationally based constraint of the effective RF by aerosol–cloud interactions (e.g., Quaas 2015) and, at the same time, to better understand the processes relevant for F_{aer}.

Acknowledgments. We thank the climate modeling community, PCMDI, and ESGF/WCDC for the CMIP5 results and are grateful to the Climate Research Unit (CRU), University of East Anglia, for providing the temperature observations. We thank Robert Pincus for valuable comments on this study. This work was funded by an ERC starting grant (''QUAERERE'', GA 306284). We thank Bjorn Stevens, Stephanie Fiedler, Stefan Kinne, and an anonymous reviewer for their help in clarifying and improving the manuscript.

REFERENCES

Boucher, O., and Coauthors, 2013: Clouds and aerosols. *Climate Change 2013: The Physical Science Basis*, T. F. Stocker et al., Eds., Cambridge University Press, 571–658.

Cherian, R., J. Quaas, M. Salzmann, and M. Wild, 2014: Pollution trends over Europe constrain global aerosol forcing as simulated by climate models. *Geophys. Res. Lett.*, **41**, 2176–2181, doi:10.1002/2013GL058715.

Ekman, A. M. L., 2014: Do sophisticated parameterizations of aerosol-cloud interactions in CMIP5 models improve the representation of recent observed temperature trends? *J. Geophys. Res. Atmos.*, **119**, 817–832, doi:10.1002/2013JD020511.

Forster, P. M., T. Andrews, P. Good, J. M. Gregory, L. S. Jackson, and M. Zelinka, 2013: Evaluating adjusted forcing and model spread for historical and future scenarios in the CMIP5 generation of climate models. *J. Geophys. Res. Atmos.*, **118**, 1139–1150, doi:10.1002/jgrd.50174.

Ghan, S. J., S. J. Smith, M. Wang, K. Zhang, K. Pringle, K. Carslaw, J. Pierce, S. Bauer, and P. Adams, 2013: A simple model of global aerosol indirect effects. *J. Geophys. Res. Atmos.*, **118**, 6688–6707, doi:10.1002/jgrd.50567.

Lamarque, J.-F., and Coauthors, 2010: Historical (1850–2000) gridded anthropogenic and biomass burning emissions of reactive gases and aerosols: Methodology and application. *Atmos. Chem. Phys.*, **10**, 7017–7039, doi:10.5194/acp-10-7017-2010.

Morice, C. P., J. J. Kennedy, N. A. Rayner, and P. D. Jones, 2012: Quantifying uncertainties in global and regional temperature change using an ensemble of observational estimates: the HadCRUT4 dataset. *J. Geophys. Res.*, **117**, D08101, doi:10.1029/2011JD017187.

Pincus, R., P. M. Forster, and B. Stevens, 2016: The Radiative Forcing Model Intercomparison project (RFMIP): Experimental protocol for CMIP6. *Geosci. Model Dev.*, **9**, 3447–3460, doi:10.5194/gmd-9-3447-2016.

Quaas, J., 2015: Approaches to observe effects of anthropogenic aerosols on clouds and radiation. *Curr. Climate Change Rep.*, **1**, 297–304, doi:10.1007/s40641-015-0028-0.

——, O. Boucher, N. Bellouin, and S. Kinne, 2008: Satellite-based estimate of the direct and indirect aerosol climate forcing. *J. Geophys. Res.*, **113**, D05204, doi:10.1029/2007JD008962.

Rotstayn, L. D., M. A. Collier, D. T. Shindell, and O. Boucher, 2015: Why does aerosol forcing control historical global-mean surface temperature change in CMIP5 models? *J. Climate*, **28**, 6608–6625, doi:10.1175/JCLI-D-14-00712.1.

Schwartz, S. E., 2012: Determination of Earth's transient and equilibrium climate sensitivities from observations over the twentieth century: Strong dependence on assumed forcing. *Surv. Geophys.*, **33**, 745–777, doi:10.1007/s10712-012-9180-4.

Unauthenticated | Downloaded 07/27/22 06:04 AM UTC

Sherwood, S. C., S. Bony, O. Boucher, C. Bretherton, P. M. Forster, J. M. Gregory, and B. Stevens, 2015: Adjustments in the forcing-feedback framework for understanding climate change. *Bull. Amer. Meteor. Soc.*, **96**, 217–228, doi:10.1175/BAMS-D-13-00167.1.

Stevens, B., 2015: Rethinking the lower bound on aerosol radiative forcing. *J. Climate*, **28**, 4794–4819, doi:10.1175/JCLI-D-14-00656.1.

——, S. Fiedler, S. Kinne, K. Peters, S. Rast, J. Müsse, S. J. Smith, and T. Mauritsen, 2017: Simple plumes: A parameterization of anthropogenic aerosol optical properties and an associated Twomey effect for climate studies. *Geosci. Model Dev.*, **10**, 433–452, doi:10.5194/gmd-2016-189.

Taylor, K. E., R. J. Stouffer, and G. A. Meehl, 2012: An overview of CMIP5 and the experiment design. *Bull. Amer. Meteor. Soc.*, **93**, 485–498, doi:10.1175/BAMS-D-11-00094.1.

Wang, C., 2015: Anthropogenic aerosols and the distribution of past large-scale precipitation change. *Geophys. Res. Lett.*, **42**, 10 876–10 884, doi:10.1002/2015GL066416.

Unauthenticated | Downloaded 07/27/22 06:04 AM UTC